

# Anodization of Gold in Oxalate Solution To Form a Nanoporous Black Film\*\*

Kazuyuki Nishio\* and Hideki Masuda

Gold nanostructures have been attracting increasing interest because they exhibit unique catalytic, optical, and biochemical properties resulting from their small feature sizes.<sup>[1]</sup> Gold colloids, which are usually formed by the reduction of gold ions in aqueous  $\text{HAuCl}_4$  solution, are a typical configuration of gold nanostructures.<sup>[2]</sup> However, gold colloids are not useful in some cases, particularly when dry conditions are required. Recently, a dealloying method in which spongelike nanoporous gold is formed through the chemical or electrochemical dissolution of less noble metals in gold alloys has been intensively studied.<sup>[3]</sup> Even though dealloying enables the spontaneous formation of nanostructures directly on a bulk surface, its application is restricted owing to the difficulty in preparing a compositionally and crystallographically homogeneous alloy and to the possible contamination by alloying metals. Therefore, the spontaneous formation of gold nanostructures on pure gold is a desirable process for expanding the application of gold nanostructures.

Anodization is an attractive method for obtaining unique fine structures on a metal electrode through the oxidation of the electrode and the reaction with the electrolyte under a positive electric field. Anodization enables the spontaneous formation of nanopores with high aspect ratios on specific metals classified as valve metals.<sup>[4]</sup> However, we found that a nanoporous film is formed by the anodization of pure gold, which has the highest standard redox potential among metals. Although the properties of gold electrodes under anodic polarization have been widely studied, previous studies have focused on the formation of thin oxide films,<sup>[5]</sup> the adsorption of anions,<sup>[6]</sup> and the synthesis of hydrocarbons,<sup>[7]</sup> not on the three-dimensional structures on a gold surface. To our knowledge, this is the first report on the formation of a nanoporous structure from pure gold. Herein, we describe the fabrication of nanoporous black films by the anodization of gold in oxalate-containing solutions. The development of nanopores on a gold anode can be explained by the formation

of a carbonaceous passivation film and the subsequent breakdown of the film on the nanoscopic scale.

Figure 1 shows representative results for the anodization of gold in oxalic acid. In this case, the potential was linearly

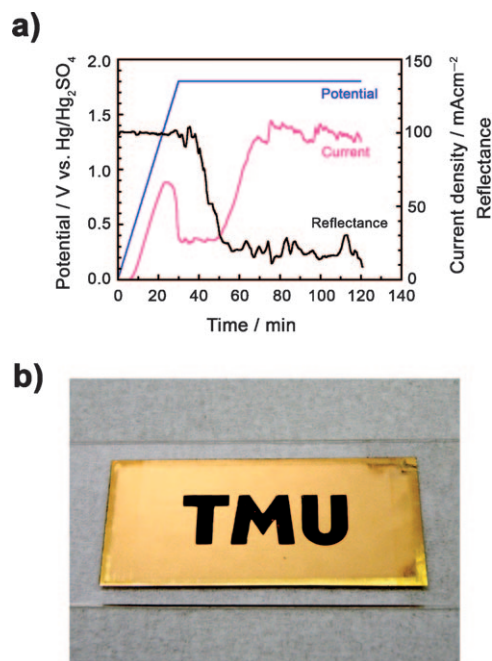


**Figure 1.** a) Controlled potential (blue), resulting current curve (red), and change in reflectance at  $\lambda = 570$  nm (black) during the anodization of gold in 0.3 M oxalic acid at 0°C. b) Photograph showing a gold foil after anodization. The size of the gold foil is  $4.5 \times 2.0$  cm.

swept from 0 to 1.8 V versus  $\text{Hg}/\text{Hg}_2\text{SO}_4$  at a rate of  $1 \text{ mV s}^{-1}$  and then retained at 1.8 V for 90 min (blue line in Figure 1 a). Under these anodizing conditions, two characteristic behaviors were observed in the current curve (red line in Figure 1 a). First, the anodic current sharply decreased during the potential sweep. The charge during the potential sweep up to 1.8 V was  $58 \text{ C cm}^{-2}$ , which is much higher than that needed to form a  $\text{Au-O}$  or  $\text{Au-OH}$  layer (ca.  $1 \times 10^{-3} \text{ C cm}^{-2}$  for a monolayer).<sup>[8]</sup> Second, the current increased roughly threefold while the potential was retained at 1.8 V. These behaviors were reproducible and unique to oxalic acid, as they have not been observed in other carboxylic acids. It was also confirmed that the potential at which the decrease in current occurs (hereafter, current-decrease potential) negatively shifts when the electrolyte is aged by repeated use. The reflectance of the gold anode was also measured during the anodization (black line in Figure 1 a). The result indicates that blackening starts

[\*] Prof. Dr. K. Nishio, Prof. Dr. H. Masuda  
 Department of Applied Chemistry  
 Graduate School of Urban Environmental Sciences  
 Tokyo Metropolitan University  
 1-1 Minamiosawa, Hachioji, Tokyo 192-0397 (Japan)  
 Fax: (+81) 42-677-2841  
 E-mail: k-nishio@tmu.ac.jp

[\*\*] We would like to thank Dr. Yoshitoki Iijima and Masahide Shima (JEOL, Ltd.) for carrying out the XPS depth investigation and AES and Yoshinari Misaki (Tokyo Metropolitan University) for performing the high-resolution TEM and EDS investigations.

Supporting information for this article is available on the WWW under <http://dx.doi.org/10.1002/anie.201005700>.

after the potential reaches 1.8 V and almost terminates before the threefold increase in current. When the potential was held at the current-decrease potential, no changes such as blackening or active dissolution were observed on the gold surface. Figure 1 b shows a photograph of a gold foil after anodization. The anodized area (the letters "TMU") uniformly turned glossy black and remained unchanged after the anodization.

Figure 2 shows scanning electron microscopy (SEM) images of the black films prepared at 1.8 V with retention times of 18 min (Figure 2a,b) and 90 min (Figure 2c,d). In

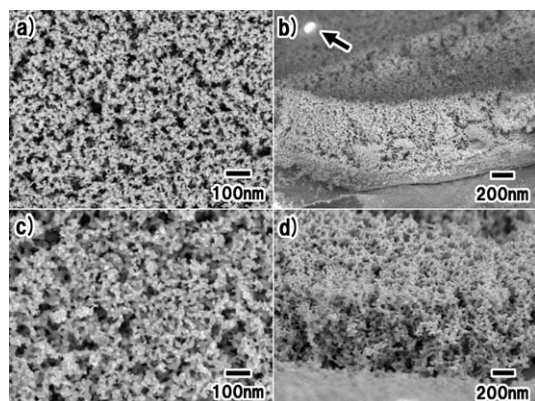


**Figure 2.** SEM images of black films prepared by anodization of gold at 1.8 V in oxalic acid. a) Surface and b) cross-sectional images of a film prepared at 1.8 V with a retention time of 18 min. c) Surface and d) cross-sectional images of a film prepared at 1.8 V with a retention time of 90 min. Other anodizing conditions were the same as those in Figure 1 a. The arrow in (b) indicates a particle of alumina, which was used for polishing gold.

the case of the retention time of 18 min, anodization was terminated after the blackening but before the threefold increase in current. The surface view in Figure 2a reveals that the black film consists of numerous fine pores typically smaller than 20 nm. It was also confirmed from the cross-sectional view (Figure 2b) that a spongelike nanoporous film with a thickness of approximately 1  $\mu\text{m}$  uniformly grew on the gold anode. Such a fine porous film remained basically unchanged after the threefold increase in current, although the film had a slightly rougher surface and framework (Figure 2c,d). As a result of the formation of the highly porous structure, the mechanical strength of the gold surface decreased. Physical contact with the film (such as touching with a finger) caused the collapse of the nanopores.

A fine particle of alumina, which was used for polishing gold (ca. 0.1  $\mu\text{m}$ ), was observed on the porous film, as marked by the arrow in Figure 2b. Alumina particles were also observed on the surface after the anodization at 1.8 V for 90 min. These results indicate that the surface of the gold anode was retained after the anodization; thus, nanopores emerged on the gold surface and then penetrated into the foil. The configuration of the nanoporous film was not affected by the crystalline orientation of gold, because the nanoporous structure was uniform over the entire polycrystalline gold anode. The glossy black color probably originates from the strong absorption of incident light by the highly porous

configuration. Within our study, the anodization of gold in other carboxylic acids<sup>[9]</sup> or sulfuric acid led to the formation of finer nanoporous films. Such films were different in many aspects from the film obtained in oxalic acid. The results will be reported elsewhere.

When deep pores are formed in a metal during anodization, a porous layer is fully oxidized or pore walls are effectively passivated against the dissolution of the metal. At the same time, the bottoms of the pores should retain their electrochemical activity. To investigate the chemical properties of the nanoporous black film, X-ray photoelectron spectroscopy (XPS) was carried out. Figure 3 shows the

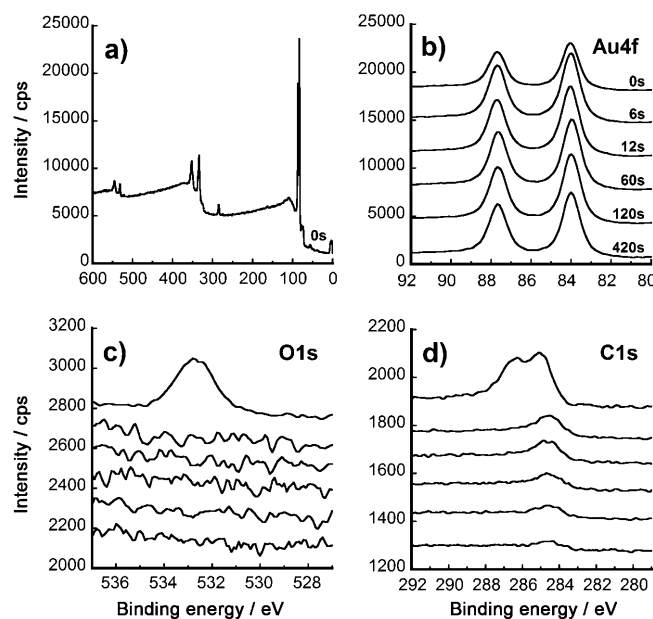


**Figure 3.** XPS spectra of a nanoporous black film: a) as-anodized sample over a wide range of binding energies, and depth profiles of b) Au 4f, c) O 1s, and d) C 1s after  $\text{Ar}^+$  ion sputtering for 0 (top) to 420 s (bottom). The anodizing conditions were the same as those in Figure 1 a. The gold substrate under the nanoporous film was not exposed to air, even after sputtering for 420 s. The measurement was carried out about two weeks after the anodization.

XPS spectra of the nanoporous black film and the depth profiles of Au 4f, O 1s, and C 1s. From the Au 4f spectra (Figure 3b), the possibility of the formation of a gold oxide film was excluded because the Au 4f peaks exhibited no chemical shift from the zero-valent state (87.7 and 84.0 eV for  $4f_{5/2}$  and  $4f_{7/2}$ , respectively). We also investigated the surface of a fresh nanoporous film (measured approximately 1 h after the anodization) and confirmed that gold oxide such as trivalent  $\text{Au}_2\text{O}_3$  (85.9 eV for  $4f_{7/2}$ )<sup>[10]</sup> does not exist even on the fresh film (Figure S1 in the Supporting Information). Additional XPS depth profiling of a polished gold foil revealed that the XPS characteristics of O and C on the nanoporous film are almost identical to those on the polished gold (Figure S2 and Table S1 in the Supporting Information). Contaminants composed of carbon and oxygen were produced during the polishing using alumina pastes and cotton buds (Figure S3 in

the Supporting Information). A considerable amount of carbon was also detected on the as-received gold foil. Therefore, the determination of the carbon content on the nanoporous film was not accomplished by XPS.

Figure 4a shows a high-resolution transmission electron microscopy (TEM) image of a nanoporous gold membrane. The TEM sample was prepared by the anodization of a thin gold film (approximately 60 nm) on a titanium substrate and the subsequent detachment of the anodized film from the substrate. Polishing was eliminated in this process. The process enabled the TEM observation of as-anodized nanopores without the need to fill them with reinforcing resin. As shown in Figure 4a, no adsorbate was observed on pore walls. However, the elemental point analysis of pore walls by energy dispersive spectroscopy (EDS) detected carbon (typically 27 at. %) and oxygen (5 at. %) in addition to gold (67 at. %) and contaminant titanium (1 at. %; Figure 4b). For reference, we analyzed the edge of a hole in a fine TEM grid (2000 mesh, Ni) that supports the nanoporous gold membrane in Figure 4.

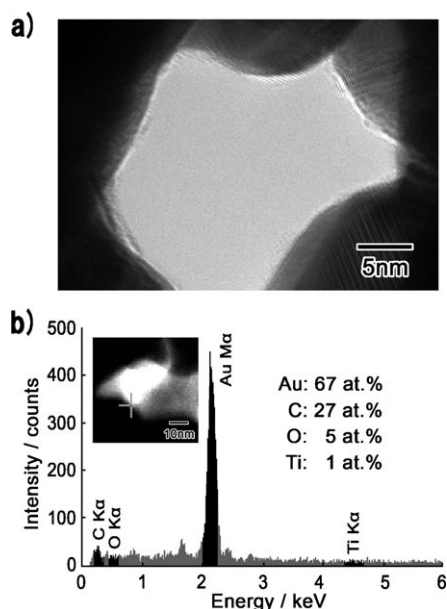


**Figure 4.** a) High-resolution TEM image of a nanoporous membrane obtained by anodization of a thin gold film on Ti. b) Typical EDS spectra of the nanoporous membrane on a pore wall (marked by a cross in the inset scanning TEM image).

The maximum concentrations of C and O at that point were 5.0 and 0.2 at. %, respectively (Figure S4 in the Supporting Information). This result suggests that C and O on the pore walls of nanoporous gold are not from the contaminant but from the adsorbate formed during the anodization in oxalic acid. Since gold does not alloy with carbon at around room temperature,<sup>[11]</sup> the EDS results imply that carbonaceous adsorbate exists as a very thin film on pore walls and thus cannot be observed directly by TEM.

On the basis of the XPS and EDS results, we consider the reasons for the characteristic behaviors of the anodic current in Figure 1a to be as follows: The marked decrease in current during the potential sweep is due to the passivation of the gold

anode. However, in our study, the common active dissolution and the subsequent oxidation of the metal surface are not involved in the process, but electrolytically generated carbonaceous matter adsorbs onto the gold. The passivation film is broken down at a higher potential (approximately 1.8 V), and pores emerge at the breakdown sites, which are nanoscopically distributed on the surface. The nanopores then penetrate into the gold anode with the successive passivation of pore walls. The threefold increase in current, which occurs after the formation of a nanoporous film, is presumably caused by the propagation of breakdown sites from their bottoms to the deep part of the nanopores. In our study, the thickness of the nanoporous film saturated at approximately 1  $\mu\text{m}$ . This effect is probably due to the insufficient passivation of pore walls in deeper regions.

Another characteristic finding of the present study is that nanopores grow on a gold anode even if the oxalate solution is neutral or alkaline. Figure 5a shows a cross-sectional SEM image of a nanoporous black film obtained by anodization in neutral sodium oxalate solution. This result demonstrates that the acidification of the electrolyte is not necessary for the growth of nanopores on gold. Furthermore, a nanoporous black film was formed in alkaline oxalate solution. Figure 5b shows the dependence of the potential-current ( $V$ - $I$ ) curve on the pH value of 0.1 M oxalate solution at 20 °C. The current-decrease potential negatively shifts with increasing pH value, as was observed when an oxalic acid electrolyte was aged by repeated use. The result in Figure 5b suggests that the formation rate and adsorption efficiency of the carbonaceous matter increases in the absence of protons. Therefore, we speculated that cathodic reaction in which oxalic acid is

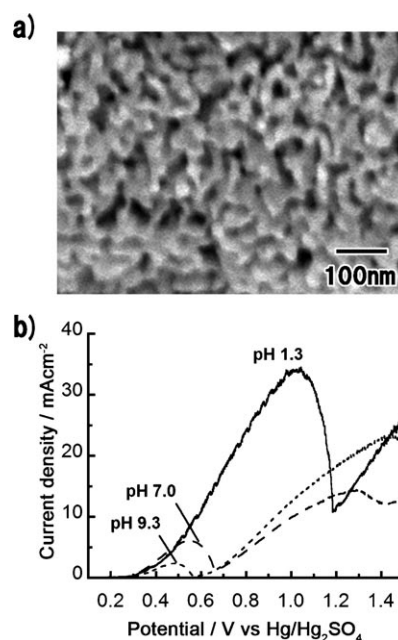


**Figure 5.** a) Cross-sectional SEM image of nanoporous gold film obtained by anodization in neutral 0.25 M sodium oxalate at 0 °C. b) Dependence of the  $V$ - $I$  curve on the pH value of 0.1 M oxalate solution at 20 °C; pH values of 1.3, 7.0, and 9.3 under an anodic sweep rate of 1  $\text{mVs}^{-1}$ .

reduced to glyoxylic acid or glycolic acid<sup>[12]</sup> might contribute to the formation of a carbonaceous film on the gold anode.

To investigate the influence of cathode products on the formation of nanoporous gold, we set a diaphragm plate in a beaker to prevent the transfer of the cathode products to the gold anode. Figure 6 shows the  $V$ - $I$  curves of five consecutive

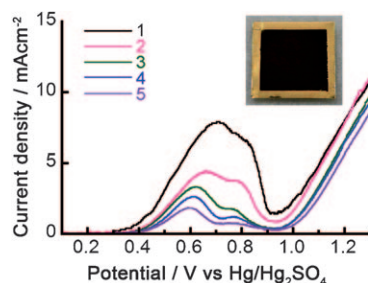


**Figure 6.**  $V$ - $I$  curves of five consecutive anodizations in 0.1 M oxalic acid at 20 °C using a diaphragm plate. The inset shows a photograph of the nanoporous gold foil ( $1 \times 1 \text{ cm}^2$ ) obtained by the first anodization up to 3.0 V.

anodizations in 0.1 M oxalic acid at 20 °C using the diaphragm plate. Figure 6 reveals that a decrease in the anodic current occurs and nanoporous black film is obtained without cathode products. The peak current markedly decreased with repeated anodization, although both pH value (1.3) and conductivity ( $235 \text{ mS m}^{-1}$ ) remained unchanged over the five consecutive anodizations. This behavior is probably due to the accumulation of carbonaceous adsorbate in the anode solution. However, the formation reaction of the carbonaceous adsorbate seems complicated and cannot be explained at present since oxalic acid is the simplest carboxylic acid and has no hydrocarbon chain. The elucidation of the reaction mechanism will be the subject of a future study.

In summary, the anodization of pure gold in oxalic acid solution enabled the formation of a nanoporous glossy black film with a thickness of approximately  $1 \mu\text{m}$ . The film had a spongelike porous configuration with a uniform hole size of about 20 nm. It was also confirmed that acidification is not necessary for the formation of nanoporous gold. Although the formation mechanism has not been clarified yet, from the results of our investigations including XPS, TEM, and EDS, we suggest that nanopores grow on a gold anode through the breakdown of a carbonaceous passivation film formed by the anodic reaction of oxalate ions. The present process is expected to be applied in various research fields, because a uniform nanoporous film with a large surface area can now be directly and readily formed on the noblest metal<sup>[13]</sup> by anodization, which can be described as a spontaneous top-down process.

### Experimental Section

A polycrystalline gold foil (Nilaco, 0.05 mm thick, 99.95 % purity) was polished using alumina pastes of different particle sizes (Baikalox, 3.0, 0.3, and 0.1  $\mu\text{m}$ ) and cotton buds (Johnson & Johnson). Anodization was conducted in a 500 mL beaker with a magnetic stirrer using a

three-electrode system with a potentiostat (Toho Technical Research PS-14) and a function generator (Toho Technical Research FG-02). The temperature of the electrolyte was controlled using a water bath equipped with a thermostatic system (Eyela CTP-1000). Potential and current were acquired as a function of time using a data logger (Yokogawa XL100). Electrochemical experiments were carried out using a  $\text{Hg}/\text{Hg}_2\text{SO}_4$  reference electrode (BAS RE-2C) to prevent the gold electrode from being attacked by chloride ions. All the potentials are given with respect to the  $\text{Hg}/\text{Hg}_2\text{SO}_4$  electrode (+0.64 V vs. standard hydrogen electrode at 25 °C). A carbon plate was used as the counterelectrode. In situ reflection measurement ( $\lambda = 570 \text{ nm}$ ) was performed using an optical spectrometer (Ocean Optics USB-2000) with an optical fiber whose tip was placed in front of the gold anode. In this system, the emergence of small gas bubbles on the anode did not affect the reflectance. After the anodization, the samples were carefully washed with distilled water.

The structure of the nanoporous film was observed using SEM (JEOL JSM-6700F) and TEM (JEOL JEM-3200FS) equipped with EDS (JEOL JED-2300T). In the SEM observation of the cross section, the anodized sample was fractured to investigate the internal structure of the nanoporous film. The thin nanoporous gold membrane used for TEM observation was prepared by the anodization of a sputter-deposited gold film. Gold (99.99 %) with a thickness of approximately 60 nm was deposited on a titanium sheet (99.5 %) using a sputtering apparatus (Eiko IB-3). During the anodization of the sample, nanopores penetrated the thin gold film. The underlying Ti was also anodized after the penetration, but its reaction rate was very low (less than  $0.05 \text{ mA cm}^{-2}$  at 1.8 V for a bare Ti sheet in 0.3 M oxalic acid at 0 °C). After the anodization, the nanoporous gold film was mechanically detached from the Ti substrate by spraying distilled water onto the sample and then fixed on a TEM grid (Gilder Grids, G2000HS-Ni). The size of the incident beam for EDS point analysis was approximately 1 nm.

An XPS depth investigation was performed with a JEOL JPS-9200 spectrometer. The anodized sample used for the XPS investigation was kept in ultrapure water until the measurement to prevent contamination from air. An SEM image and Auger electron spectra of the contaminant on a polished gold foil were obtained using a JEOL JAMP-9500F instrument. Oxalate solutions (0.1 M) with pH values of 1.3 and 7.0 were prepared as 0.1 M oxalic acid and sodium oxalate, respectively. Alkaline 0.1 M oxalate solution (pH 9.3) was prepared by increasing the pH value of 0.1 M sodium oxalate by adding a small amount of NaOH solution. In the anodization with a diaphragm plate, a 1000 mL plastic beaker without a stirring apparatus was used. The anode and cathode cells were separated with a fused alumina diaphragm plate, an acrylic supporting plate, and epoxy resin. The sweep rate was  $1 \text{ mV s}^{-1}$ , and a new gold foil was used for each anodization.

Received: September 11, 2010

Revised: November 2, 2010

Published online: January 12, 2011

**Keywords:** anodization · carboxylic acids · gold · nanoporous materials · nanostructures

- [1] a) M. Haruta, *Chem. Rec.* **2003**, 3, 75; b) T. Ishida, M. Haruta, *Angew. Chem.* **2007**, 119, 7288; *Angew. Chem. Int. Ed.* **2007**, 46, 7154; c) A. Henglein, *Langmuir* **1999**, 15, 6738; d) P. V. Kamat, *J. Phys. Chem. B* **2002**, 106, 7729; e) C. A. Mirkin, R. L. Letsinger, R. C. Mucic, J. J. Storhoff, *Nature* **1996**, 382, 607.
- [2] G. Schmid, *Chem. Rev.* **1992**, 92, 1709, and references therein.
- [3] a) J. P. Candy, P. Fouilloux, M. Keddah, H. Takenouti, *Electrochim. Acta* **1981**, 26, 1029; b) R. Li, K. Sieradzki, *Phys. Rev. Lett.* **1992**, 68, 1168; c) J. Erlebacher, M. J. Aziz, A. Karma, N. Dimitrov, K. Sieradzki, *Nature* **2001**, 410, 450; d) M. B. Cortie,

- A. I. Maarouf, G. B. Smith, *Gold Bull.* **2005**, 38, 14; e) J. Biener, A. M. Hodge, A. Hamza, *Appl. Phys. Lett.* **2005**, 87, 121908; f) C. A. Volkert, E. T. Lilleodden, D. Kramer, J. Weissmüller, *Appl. Phys. Lett.* **2006**, 89, 061920.
- [4] a) F. Keller, M. S. Hunter, D. L. Robinson, *J. Electrochem. Soc.* **1953**, 100, 411; b) H. Masuda, K. Fukuda, *Science* **1995**, 268, 1466; c) J. M. Macak, H. Tsuchiya, L. Taveira, S. Aldabergerova, P. Schmuki, *Angew. Chem.* **2005**, 117, 7629; *Angew. Chem. Int. Ed.* **2005**, 44, 7463; d) H. Tsuchiya, J. M. Macak, I. Sieber, P. Schmuki, *Small* **2005**, 1, 722.
- [5] B. E. Conway, *Prog. Surf. Sci.* **1995**, 49, 331, and references therein.
- [6] a) K. Katoh, G. M. Schmid, *Bull. Chem. Soc. Jpn.* **1971**, 44, 2007; b) D. S. Corrigan, P. Gao, L. W. H. Leung, M. J. Weaver, *Langmuir* **1986**, 2, 744; c) S. Bilgic, M. Kabasakaloglu, *Chim. Acta Turc.* **1986**, 14, 23; d) S. Floate, M. Hosseini, M. R. Arshadi, D. Ritson, K. L. Young, R. J. Nichols, *J. Electroanal. Chem.* **2003**, 542, 67.
- [7] a) H. Kolbe, *Ann. Chem. Pharm.* **1849**, 69, 257; b) T. Dickinson, W. F. K. Wynne-Jones, *Trans. Faraday Soc.* **1962**, 58, 382; c) B. E. Conway, M. Dzieciuch, *Can. J. Chem.* **1963**, 41, 21; d) B. E. Conway, M. Dzieciuch, *Can. J. Chem.* **1963**, 41, 38; e) B. E. Conway, M. Dzieciuch, *Can. J. Chem.* **1963**, 41, 55; f) N. Sato, T. Sekine, K. Sugino, *J. Electrochem. Soc.* **1968**, 115, 242.
- [8] G. M. Schmid, R. N. O'Brien, *J. Electrochem. Soc.* **1964**, 111, 832.
- [9] K. Nishio, H. Masuda US Pat. 20100230287, **2010**.
- [10] T. Dickinson, A. F. Povey, P. M. A. Sherwood, *J. Chem. Soc. Faraday Trans. 1* **1975**, 71, 298.
- [11] R. B. McLellan, *Scr. Metall.* **1969**, 3, 389.
- [12] a) J. Tafel, G. Friedrichs, *Ber. Dtsch. Chem. Ges.* **1904**, 37, 3187; b) D. J. Pickett, K. S. Yap, *J. Appl. Electrochem.* **1974**, 4, 17; c) F. Goodridge, K. Lister, R. E. Plimley, K. Scott, *J. Appl. Electrochem.* **1980**, 10, 55.
- [13] B. Hammer, J. K. Nørskov, *Nature* **1995**, 376, 238.